IMPROVEMENT OF THE EFFICIENCY OF DIFFUSER FLOW BY MEANS OF REGULAR VORTICES

V. K. Migai,* Yu. A. Kravtsov,
V. B. Dovzhik, and I. V. Zhitomirskaya

UDC 532.54:519.63

The effect of the positive action of localized vortex formations on the flow in separation diffusers is considered. The analysis uses the mathematical model of an elementary vortex diffuser based on the Navier–Stokes equations for an incompressible, viscous liquid with effective turbulent viscosity. The finite-difference method of fractional steps, amounting to trial runs, is used to obtain the solution. Calculations of the flow in a flat channel with a step widening, where ribs of various length are mounted in the direction across the flow, are performed. The drag and recovery coefficients as functions of the rib length and location are determined.

The positive effect of localized vortex formations on the flow in separation diffusers was first used in [1, 2]. The designs proposed in these papers formed a basis for the development of a new class of diffusers, called vortex diffusers (they are referred to as VCD – Vortex Controlled Diffusers – in the literature published abroad) (Fig. 1). The main idea [1] of Ringleb's diffuser design (Fig. 1a) consists in providing conditions where stable vortices develop and are maintained within cavities, which should help drive the main flow toward expansion, reduce the separation zone, and lower the diffuser drag. On the basis of two-dimensional potential flow with two positive vortices, Ringleb derived a function for conformal mapping of the region of such a diffuser to the upper half-plane with two singularities. Thus, the equilibrium conditions for steady-state vortices in cavities and a simple scheme for calcualting the flow ere obtained. However, the proposed calculation scheme entailed discrepancies with experimental data. Great difficulties were experienced in ensuring vortex stability in the cavities of such diffusers, which constituted their considerable and decisive disadvantage.

A characteristic feature of the diffuser proposed in [2] (Fig. 1b) is the presence of a recessed system of transverse ribs on the bounding walls. As was demonstrated in [3], the positive effect is determined by the presence of regular vortices in grooves and a higher degree of turbulence in the boundary region. With such ribbing, the optimum results according to [3] are obtained for a groove width b = 1-5 mm, the depth-to-width ratio of the grooves a/b = 2, and a diffuser flare angle β = 35-50° (the beginning of the groove system must lie in the pre-separation region). For large flare angles, the efficiency of a diffuser provided with ribbing increases by a factor of up to 2.5. A diffuser with transverse baffles [4] (Fig. 1c) constitues a variant of such diffusers. These diffusers differ from those with ribbing by the fact that the width and depth of the cavities are larger by one order of magnitude than those in ribbed diffusers (macroribbing versus microribbing). As was shown in [4], the higher efficiency of such diffusers is determined by the breakup of large vortices by the transverse baffles into a system consisting of several small, regular vortices, which entails smaller losses than a system of one or two large vortices produced by the step widening (without baffles).

Reports on new designs of round vortex diffusers appeared in 1975-1980. They were investigated under the supervision of Adkins (Great Britain) at the Krepfield Technological

*Deceased.

I. I. Polzunov Central Boiler and Turbine Institute, Leningrad. Translated from Inzhenerno-Fizicheskii Zhurnal, Vol. 58, No. 5, pp. 737-742, May, 1990. Original article submitted February 28, 1989.

 0022-0841/90/5805-0562$12.50

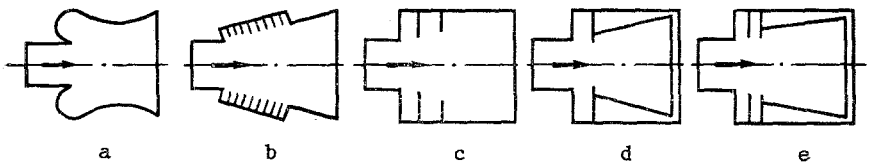

Fig. 1. Schematic diagrams of diffusers with regular vortices. a) Ringleb diffuser [1]; b) ribbed diffuser [2]; c) ribbed diffuser [4]; d) Adkins diffuser [5]; e) simulated diffuser [6].

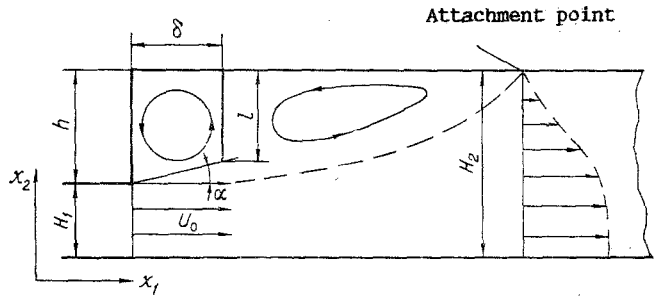

Fig. 2. Schematic of the theoretical diffuser with a baffle.

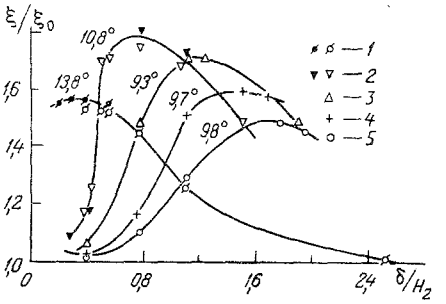

Fig. 3. Relative recovery coefficient in a channel with step expansion as a function of the baffle location. 1) ℓ/H_2 = 0.58; 2) 0.53; 3) 0.47; 4) 0.42; 5) 0.36.

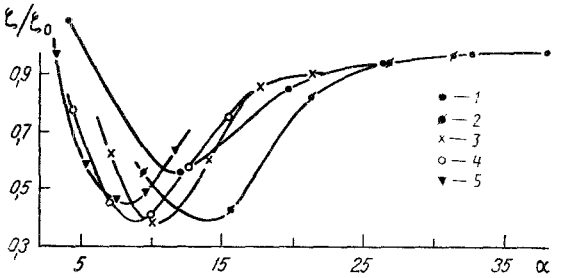

Fig. 4. Relative drag coefficient for a channel with step expansion and a single baffle as a function of the angle α. 1) δ/H_2 = 0.39; 2) 0.50; 3) 0.78; 4) 1.11; 5) 1.50; α (deg).

Institute and at the Rolls Royce Company (Fig. 1d) [5]. In such a diffuser, a cavity containing a localized vortex is formed beyond the step widening. A smooth, rectilinear diffuser with a vortex generator is provided beyond this vortex chamber. A pre-diffuser is mounted ahead of the vortex chamber in a number of Adkins' designs. Investigations [5] have shown that, for divergence ratios of 2 and 2.5, the coefficient of static pressure recovery is higher by 20-30% than in the case of an ordinary diffuser of the same length and with the same divergence ratio. It was also found that static pressure recovery to the same degree is secured in a composite diffuser over a length approximately one half as large as that in a diffuser of the usual design.

The single vortex chamber in the composite diffuser was replaced by a double vortex chamber in [6] (Fig. 1e), which helped increased the efficiency by 20%.

These results were obtained experimentally without any analytical investigations of such vortex diffusers.

The possibility of improving the efficiency ofdiffuser devices by using regular vortices, produced by transverse baffles, is demonstrated below by a numerical investigation of the flow of an incompressible, viscous liquid in a flat channel with the stepped divergence ratio $n = F_{out}/F_{in} = 3$ (Fig. 2).

We varied the baffle length and the distance from the step to the baffle in our calculations.

The flow is assumed to be turbulent. The flow is described by the Navier–Stokes equations, where the variable has the direction of the inlet velocity with the effective viscosity ν_{eff}. In a Cartesian coordinate system, the simultaneous system with the continuity equation is given by

$$\sum_{k=1}^{2}\left(u_k\frac{\partial u_i}{\partial x_k}-\frac{\partial}{\partial x_k}\nu_{\text{eff}}\frac{\partial u_i}{\partial x_k}\right)+\frac{\partial P}{\partial x_i}=0,\ i=1,\ 2;\ \sum_{k=1}^{2}\frac{\partial u_k}{\partial x_k}=0. \tag{1}$$

The assigned conditions are a uniform velocity profile at the channel inlet, nonleakage and slippage at the solid surfaces, and soft boundary conditions at the outlet.

The effective viscosity is assumed to be constant over the transverse cross section of the channel and variable along its length. It was calculated along the segment preceding the step on the basis of Laufer's data [7] for a tube. It was equal to $\nu_{in}/U_0H_2 = 0.00035$, which corresponded to the effective Reynolds number $Re_{eff} = 2850$. It was assumed that this viscosity persists to a distance equal to the opening diameter d due to the jet inertia, beyond which it increases linearly to the end of the initial section of the jet $x_1 = 8d$, after which it remains constant ($\nu_{out}/U_0H_2 = 0.11$).

In view of the absence of reliable experimental data on the coefficient of turbulent viscosity in such structures, the accuracy of the ν_{eff} value was determined indirectly with respect to the extent of the return flow zone, which amounted to 7h (h is the step height) in experimental determinations for n = 3 [8]. The value $\nu_{out}/H_0H_2 = 0.011$ was obtained on the basis of this condition. The theoretical coefficient of total head loss from the opening to the point of attachment (to the end of the reverse flow zone) was equal to $\zeta_0 = 0.394$. This is in satisfactory agreement with the Borda–Carnot equation, derived from the condition of absence of friction at the channel walls with an allowance for nonuniformity of the velocity field at the outlet:

$$\zeta=\frac{2M_2-N_2}{n^2}+1-\frac{2}{n}=0{,}388,$$

where the Boussinesq coefficient M_2 and the Coriolis coefficient N_2 pertain to the transverse cross section passing through teh attachment point.

The problem was solved by using the fixing method, for which the steady-state Navier–Stokes equations were replaced with their transient-state analogs, while the additional term $1/A_p(\partial P/\partial t)$ was introduced in the continuity equation. System (1) in vector form is given by [9]:

$$A\frac{\partial f}{\partial t}+\Lambda f=0,\quad f|_{t=0}=f_0,$$

$$A=\begin{bmatrix}1&0&0\\0&1&0\\0&0&1/A_P\end{bmatrix},\quad \Lambda=\begin{bmatrix}L&0&\partial/\partial x_1\\0&L&\partial/\partial x_2\\\partial/\partial x_1&\partial/\partial x_2&0\end{bmatrix},\quad f=\begin{bmatrix}u_1\\u_2\\P\end{bmatrix},\tag{2}$$

$$L=\sum_{k=1}^{2}(u_k\,\partial/\partial x_k-\partial/\partial x_k\nu_{\text{eff}}\,\partial/\partial x_k).$$

The following system can be used as the difference analog of Eq. (2):

$$A\frac{f^{n+1}-f^n}{\tau}+\Lambda^{(s)}f^{n+1}=0,$$

where $\Lambda^{(s)}$ is the matrix difference operator, which approximates the differential operator Λ of the order s with respect to the three-dimensional step, and τ is the time step. The values of the components of vector f^{n+1} are defined as $f^{n+1}=f^n+\eta^{n+1}$, where η^{n+1} is the correction vector, which constitutes the solution of the system

$$(E+\tau A^{-1}\Lambda^{(s)})\,\eta^{n+1}=-\tau A^{-1}\Lambda^{(s)}f^n.$$

The vector η^{n+1} was determined by using the method of fractional steps, where the solution procedure is reduced to scalar trial runs.

A hybrid grid with the pressure node at the center of a cell, and the velocity nodes on its sides, was used in passing from differential equations to the finite-difference equations. With such a grid and uniform spacings, the partial derivatives in the continuity equation, the diffusion terms, and the pressure gradient are approximated with second-order accuracy with respect to the three-dimensional step. A combined difference scheme was used for the convective terms, i.e., quadratic counterflow interpolation was used for the grid Reynolds numbers $|\mathrm{Re}_g| \le 8/3$, while simple counterflow interpolation was used for $|\mathrm{Re}_g| > 8/3$; the diffusion terms were omitted.

Most of the calculations were performed by using a uniform 97 × 18 grid with the spacing $h_1 = h_2 = 1/18$. In cases where the baffle was mounted at a distance closer than $\delta/H_2 = 0.4$, a grid with variable spacing in the x_1 direction was used, in the region $0.25 < x_1/H_2 < 1.4$, the spacing was one half as large, so that not less than 10 nodes were used for the vortex arising between the step and the baffle. For comparison, some calculations for the same geometry were performed by using both uniform and nonuniform grids. Refinement of the grid does not affect the flow without baffles: The velocity fields, the drag coefficients, and the recovery coefficients do not change. The maximum deviations of these coefficients amount to 4% in calculations pertaining to baffles.

The model for which the calculations were performed is illustrated in Fig. 2. The channel height at the outlet H_2 was used as the normalizing dimension, while the inlet velocity U_0 was used at the normalizing velocity. The overall channel length was equal to 5.39 H_2. The baffle length varied within the $0.36 < \ell/H_2 < 0.64$ range, while the distance between the baffle and the step varied within the $0.2 < \delta/H_2 < 1.94$ range. It was found that, in all cases, equal diagrams of the velocity U with the Coriolis coefficient $N_2 = 2.54$ apply to the cross section passing through the attachment point. Therefore, the design efficiency was estimated with respect to the drag coefficient $\zeta = (P_2 - P_1)/0.5\rho U_0^2$ and the pressure recovery coefficient $\xi = 1 - N_2/n^2 - \zeta$ for the segment from the inlet section to the attachment point, where P_1 and P_2 are the total energies per unit discharge in the respective cross sections. In order to compare the calculation results with each other and with experimental data, the coefficients obtained were reduced to the corresponding coefficients for a channel with step expansion. For the divergence ratio $n = H_2/H_1 = 3$, they were equal to $\zeta_0 = 0.394$ and $\xi_0 = 0.324$.

Our numerical experiment has shown that there is an optimum position of the transverse baffle beyond the step, depending on the baffle length. Figure 3 shows the normalized recovery coefficient as a function of the baffle location. The relative baffle length is the parameter in this case. Such values of ℓ/H_2 are explained by the fact that only an integer number of steps can be used in varying this parameter. The dark points in the figure were obtained by calculations based on a finer grid. All curves have a clearly defined maximum. It was found that the most efficient baffle arrangement is the one which, on the one hand, does not hinder the natural expansion of the jet and, on the other, covers completely the reverse flow section.

The same figure also shows the values of the angle α (formed by the line connecting the step edge to the lower end of the baffle and the direction of the inlet velocity) ensuring the highest degree of pressure recovery with a baffle of a given length. The value of α is close to 10°.

The relative drag coefficient of the segment from the edge of the step to the attachment section as a function of the angle α is shown in Fig. 4. In the optimum case, the total head loss amounts to 40% of the loss in a channel without a baffle. This result was obtained when a baffle with a length of 0.53 H_2 was mounted at the distance $\delta/H_2 = 0.75$. This effect is somewhat stronger than that found in experiments, since calculations take into account only the loss due to vortex formation, while a segment extending the steady velocity field is considered in experiments.

The following conclusions can be drawn from the results of the numerical experiment: The effectiveness of a baffle in a channel with step expansion is determined by the distance between the baffle and the outlet edge and by the angle α. The cavity where the intermediate vortex is formed should have a shape close to a quadratic one, while the angle should be close to the flare angle of the jet (10°).

Thus, our theoretical investigation supports the experimentally determined positive effect of transverse baffles on the diffuser flow efficiency. As for the physical essence of these phenomena, it is multifaceted and still incompletely understood. With regard to a composite vortex diffuser with two chambers (see Fig. 1e), which is characterized by the maximum efficiency, the physical processes can be represented as follows: The presence of two cavities reduces the overall loss in comparison with a single cavity; due to the turbulence and the presence of regular submerged vortices, the region near the wall is characterized by elevated kinetic energy, which is utilized positively along the smooth segment, resulting in a greater pressure increase. The presence of a trransverse rib of small height at the inlet to the smooth conical segment further agitates the flow and reduces the reverse flow. Annular vortex chambers help reduce peripheral nonuniformity. All these phenomena are interconnected, which, in the final analysis, results in a higher efficiency of the diffuser device.

NOTATION

n, divergence ratio; F_{in} and F_{out}, surface areas of the inlet and the outlet cross sections, respectively; x_1 and x_2, Cartesian coordinates; u_1 and u_2, velocity components corresponding to the above coordinates, respectively; P, pressure, normalized with respect to the inlet velocity U_0; ν_{eff}, effective viscosity; H_1 and H_2, channel height at the inlet and outlet, respectively; h, step height; f, vector of the functions to be determined; η, correction vector; A_p, weighting coefficient for $\partial P/\partial t$; h_1, h_2, and τ, spatial and time steps; Re_g, grid Reynolds number; ℓ, rib length; δ, distance between the step and the rib; ξ and ζ, coefficients of recovery and drag for the segment form the step to the attachment point, respectively; M_2 and N_2, Boussinesq and Coriolis coefficients for the section passing through the attachment point, respectively.

LITERATURE CITED

1. F. O. Ringleb, Trans. ASME, Ser. D, No. 4, 127-130 (1960).
2. V. K. Migai, Énergomashinostroenie, No. 4, 21-24 (1960).
3. V. K. Migai and É. I. Gudkov, Design and Calculation of Exit Diffusers for Turbomachines [in Russian], Leningrad (1981).
4. V. K. Migai, Teploénergetika, No. 7, 16-18 (1979).
5. Adkins, Trans. ASME, Theoretical Fundamentals of Engineering Calculations, No. 3, 18-21 (1975).
6. G. I. Bogoradovskii, Yu. A. Kravtsov, V. K. Migai, et al., Teploénergetika, No. 7, 13-15 (1987).
7. J. O. Hinze, Turbulence [Russian translation], G. N. Abramovich (ed.), Moscow (1963).
8. Kim, Klein, and Johnston, Trans. ASME, Theoretical Fundamentals of Engineering Calculations, No. 3, 124-132 (1980).
9. V. B. Dovzhik and V. K. Migai, Inzh. Fiz. Zh., 55, No. 1, 42-50 (1988).